Down-tail mass loss by plasmoids in Jupiter's and Saturn's magnetospheres

S. W. H. Cowley[1,*], J. D. Nichols[1], and C. M. Jackman[2]

[1] Department of Physics and Astronomy, University of Leicester, Leicester LE1 7RH, UK

[2] Department of Physics and Astronomy, University of Southampton, Southampton SO17 1BJ, UK

Key Points:

Plasmoid mass-loss estimates at Jupiter and Saturn fall far short of moon inputs

We argue that observed events connect to far-tail structures also disconnected

Mass-loss rates are revised upward by at least an order of magnitude

Draft A: Submitted to **Journal of Geophysical Research: Space Physics**, 26 May 2015

*Corresponding author (swhc1@le.ac.uk)

Abstract Recent estimates of the plasma mass loss rates by the formation and down-tail propagation of plasmoids observed in the plasma sheet in Jupiter's and Saturn's magnetosphere fall short of inner moon source rates by at least an order of magnitude. Here we argue that on the time scale between large-scale disconnection events, ~15 h at Jupiter and ~45 h at Saturn, mass-loaded closed flux tubes will typically have stretched out a few hundred planetary radii down-tail at speeds ~100-200 km s^{-1}. Consequently, the "plasmoids" of order ~10 planetary radii in length observed at closer planetary distances represent only a small planetward portion of the overall structure that is disconnected and lost down-tail. Plasmoid mass-loss estimates are then revised upward by around an order of magnitude, becoming comparable to the moon source values. Additional "hidden", e.g., small scale, mass-loss processes of comparable strength may not then be required. This physical picture also provides a simple explanation for the asymmetry in the plasmoid bipolar field signature observed at both Jupiter and Saturn, and predicts that the apparent plasmoid length will increase with distance down-tail to a limit beyond a few hundred planetary radii where the full ~100-200 planetary radii structures will be observed.

1. Introduction

A principal feature of the outer environments of Jupiter and Saturn are the sources of gas and plasma formed by the moons Io and Enceladus, respectively, which orbit deep within the equatorial quasi-dipolar magnetospheres. At Jupiter, the neutral gas emitted by the moon Io, orbiting at a radial distance of ~6 R_J, forms a source of sulfur and oxygen plasma of typical strength ~500-1000 kg s^{-1} (within a possible range ~250-1500 kg s^{-1}) [*Thomas et al.*, 2004 and references therein; *Bagenal and Delamere*, 2011 and references therein]. (R_J is Jupiter's 1 bar equatorial radius equal to 71,492 km.) This plasma is primarily transported outward by centrifugally-driven flux tube interchange motions [e.g., *Krupp et al.*, 2004 and references therein], and must eventually be lost to the solar wind through some down-tail transport process. *Vasyliunas* [1983] proposed that closed mass-loaded flux tubes could stretch out down-tail following sub-corotating transport to the nightside though the dusk sector, and would eventually pinch off via reconnection within the plasma layer, forming a large-scale tailward-travelling closed-loop plasmoid. In principle this process can occur in a steady state as originally envisaged, but more likely proceeds in an episodic time-dependent manner, either on large spatial scales involving a significant sector cross-tail, or as a phenomenon operating on smaller length and time scales [*Kivelson and Southwood*, 2005]. In either case, this "Vasyliunas cycle" process can occur continuously with on-going "Dungey-cycle" flow driven by the solar wind [*Cowley et al.*, 2003]. Similarly at Saturn, the gas emitted by the moon Enceladus, orbiting at a radial distance of ~4 R_S, forms a source of water group plasma of likely strength ~50-150 kg s^{-1} (within a possible range ~20-300 kg s^{-1}) [*Bagenal and Delamere*, 2011 and references therein; *Chen et al.*, 2010; *Fleshman et al.*, 2013; *Thomsen et al.*, 2014]. (R_s is Saturn's 1 bar equatorial radius equal to 60,268 km.) Again, this plasma is primarily transported outwards by flux tube interchange events [e.g., *Hill et al.*, 2005; *Chen and Hill*, 2008; *Mauk et al.*, 2009 and references therein], and must eventually be lost to the solar wind primarily down Saturn's magnetospheric tail. Other sources of plasma within these systems, such as the planetary ionosphere and solar wind, are less significant in terms of mass rates by at least an order of magnitude [e.g., *Bagenal and Delamere,* 2011], and need not be considered explicitly here.

As a consequence of these expectations, interest has focused on the observation of reconnection-related plasmoid events in the nightside magnetospheres of both Jupiter and Saturn. These may be observed either directly within the plasma sheet via a bipolar signature in the transverse field with tailward flow or by a related perturbation in the tail lobe forming a "traveling compression region" (TCR), together with related field "dipolarization" events with sunward flow on the planetward side of the reconnection site. Such events have been found to be relatively common both at Jupiter [*Woch et al*., 2002; *Kronberg et al*., 2005, 2007, 2008a; *Vogt et al*., 2010, 2014], and at Saturn [*Bunce et al*., 2005; *Jackman et al*., 2007, 2008, 2011, 2014, 2015; *Hill et al*., 2008]. At Jupiter, observation of reconnection-related events is strongly biased toward the post-midnight hours, ~00-04 h local time (LT), with planetward- and tailward-directed events being separated in the equatorial plane by a line at ~90 R_J radial distance near dawn extending to ~100 R_J near midnight, thus representing the typical location of the reconnection sites. Tailward-directed plasmoid signatures are thus detected principally at and beyond these distances [*Vogt et al*., 2014]. At Saturn, reconnection-related events appear to be less biased towards the post-midnight sector, and there is no clear demarcation line between tailward- and planetward-directed events, with tailward-moving plasmoids being observed at distances typically beyond ~30-40 R_S [*Jackman et al*., 2014]. The reconnection sites thus appear to be more variably located in radial distance in this case.

Particular attention in recent studies has been placed on estimating the size, and hence mass, of the observed plasmoids, and on their frequency of occurrence, and hence the associated mass loss rate. Such estimates are clearly problematical using the single-spacecraft data presently available, principally Galileo data at Jupiter and Cassini data at Saturn. However, as will be discussed in more detail in section 2, the mass loss rates determined to date generally fall far short of those implied by the moon sources quoted above. Thus from an initial study *Bagenal* [2007] estimated a plasmoid mass loss rate at Jupiter of ~30 kg s^{-1}, while from a more detailed survey *Vogt et* *al*. [2014] determined a range ~1-120 kg s^{-1}, compared with the Io plasma source quoted above of typically ~500-1000 kg s^{-1}. Similarly, from a detailed plasmoid survey at Saturn, *Jackman et al*. [2014] estimate an associated mass loss rate of ~3 kg s^{-1}, compared with a likely Enceladus plasma source of typically ~50-150 kg s^{-1}. In both cases, these estimates thus fall short of the total mass-loss requirements by at least an order of magnitude. It has thus been suggested on this basis that some other more significant mass-loss processes is required, involving, e.g., small-scale structures that are more difficult to detect [*Bagenal*, 2007; *Kivelson and Southwood*, 2005; *Delamere and Bagenal*, 2010]. Here, however, we suggest that the basis on which the above mass-loss rates were determined may under-estimate the value by a significant factor, such that dominant alternatives of this nature may not be required. In the next section we begin by briefly reviewing the above recent mass loss rate determinations and the assumptions on which they are based.

2. Plasmoid Mass-Loss Rate Estimates

Estimates of the mass loss associated with tailward-propagating plasmoid events clearly require a determination of their size, their frequency of occurrence, and their typical interior plasma properties. The size estimate requires a determination of their down-tail length, obtained from their observed duration and down-tail speed, their thickness taken to be comparable with or a little larger than the thickness of the plasma sheet, and their cross-tail width, obtained from an interpretation of the occurrence statistics. Their frequency of occurrence is similarly obtained from the numbers observed per unit time spent within some “active region”, corresponding, e.g., to the vicinity of the plasma sheet in some defined LT sector where plasmoid events are observed. From single-spacecraft data it is of course impossible to know whether a given event spans the whole of the latter LT sector or just some fraction *f*. However, in the latter case the overall frequency of occurrence is just related to the observed frequency by the inverse factor 1/*f*, so that this drops out in estimates of the mass loss rate. Here we will assume for simplicity of argument that each observed event spans the whole LT extent of the “active regions” at Jupiter and Saturn.

2.1. Jupiter Plasmoid Estimates

In their study of 43 Jupiter plasmoid events, *Vogt et al*. [2014] determined a length of ~2.6 R_J based on a mean duration of ~7 min between extrema in the field component transverse to the plasma sheet (essentially the spherical polar θ field component B_θ), and a typical tailward speed of ~450 km s^{-1} [*Kronberg et al*., 2008a]. They recognize, however, that the distance between the B_θ extrema represents only a portion of the overall structure, such that, e.g., on the basis of the flux rope model of *Kivelson and Khurana* [1995] this may underestimate the true length by factors of up to ~8. They thus take a full length range of ~2.6-20 R_J. Similarly they take the plasmoid thickness to lie in the range ~2-12 R_J based on the results of *Khurana and Schwarzl* [2005] and *Kronberg et al*. [2008b], while for the cross-tail width they take the range ~45-70 R_J, corresponding to ~2-3 h LT at a radial distance of ~90 R_J. Following *Kasahara et al*. [2013], they further take a particle number density 0.01 cm^{-3} of mass 20 ions, though we note that *Kronberg et al*. [2008b] suggests a slightly higher value of ~0.025 cm^{-3} on the basis of the nightside thermal plasma measurements presented by *Frank et al*. [2002]. Taking the smaller and then the larger of each spatial dimension together with a number density 0.01 cm^{-3} then yields a plasmoid mass in the range ~0.03-2.1×10^6 kg. *Vogt et al*. [2014] also conclude that their occurrence statistics are consistent with a production rate of ~1 plasmoid per day, though this again could be higher by a factor of up to ~5 if a significant proportion of events are missed when the spacecraft is sufficiently displaced from the oscillating plasma sheet. With the above numbers for the mass per plasmoid, the lower production rate yields a mass loss rate in the range ~0.3-24 kg s^{-1}, while the higher rate yields a range ~2-120 kg s^{-1}, essentially as reported by *Vogt et al*. [2014] as quoted in section 1. If instead we take likely values from the above ranges of the length ~15 R_J, thickness ~7 R_J, and width ~70 R_J (in line with the assumption mentioned above), together with a slightly higher number density of 0.02 cm^{-3} and the above ion mass, we obtain a typical plasmoid mass of ~1.8×10^6 kg, and with a typical recurrence time of ~15 h we obtain a typical mass-loss rate of ~30 kg s^{-1}, similar to the initial result of *Bagenal* [2007]. Such rates clearly fall far short of the estimated Io plasma production rate of ~500-1000 kg s^{-1}, by more than an order of magnitude.

2.2. Saturn Plasmoid Estimates

Similarly, in their recent study of 99 Saturn plasmoid events, *Jackman et al*. [2014] estimate a mean plasmoid length of ~4.3 R_S, corresponding to a mean peak-to-peak field duration of ~14 min and a speed of ~300 km s^{-1}, a thickness of ~2 R_S, and the full ~90 R_S width of the tail, and combine these dimensions with an upper limit plasma number density 0.1 cm^{-3} of mass 16 ions from *Thomsen et al*. [2014] to estimate a mean plasmoid mass of ~4.5×10^5 kg. Over the full range of events they study, the masses are found to range from about an order of magnitude smaller to a factor of ~5 larger than this value. From the number of events observed within an "active region" beyond ~20 R_S and the time spent within this region (99 events in ~190 days), they also estimate a production rate of one plasmoid every ~45 h (~1.9 days), thus yielding a mass loss rate of ~3 kg s^{-1}, as they report. We again note, however, that the full length of the plasmoids may be a reasonable factor larger than the distance between the observed extrema in the B_θ field component employed in this calculation, and that the plasmoid thickness might similarly be a factor larger than that of the plasma sheet half thickness employed. If we take likely values on this basis of a length of ~15 R_S, a thickness ~7 R_S, and a width ~60 R_S (a reasonable fraction of the tail width), together with a number density ~0.03 cm^{-3} not quite at the top of the observed range and the above ion mass, we find a typical plasmoid mass of ~1.1×10^6 kg, which with the above recurrence time yields a mass loss rate of ~7 kg s^{-1}, still falling far short of the Enceladus plasma production rate of ~50-150 kg s^{-1}.

3. Modified Scenario

The above estimates are based on the assumption that the length of the observed "plasmoid" structure, determined as some modest factor times the distance between the extrema in the bipolar B_θ field perturbation, is representative of the whole of the plasma sheet that is detached and eventually lost down-tail by a given reconnection event. The above occurrence statistics strongly suggest, however, that this is not the case. Given that the time between individual events may be ~15 h at Jupiter and ~45 h at Saturn, as indicated above in section 2, the mass-loaded flux tubes will generally have extended to much larger distances down-tail than the spacecraft observation points prior to disconnection, as we will show below. When a reconnection event occurs planetward of the spacecraft, typically located at ~100 R_J at Jupiter and ~50 R_S at Saturn, the field and plasma disturbance that propagates tailward over the latter forming the observed "plasmoid" will then correspond only to the near-planet end of an overall structure disconnected by the event that extends to much larger distances down the tail. In this case, the mass-loss rates discussed in section 2 will represent significant under-estimates, as we will go on to discuss.

3.1. Down-Tail Flow of Mass-Loaded Flux Tubes

First, however, we estimate the speed of down-tail flow of mass-loaded flux tubes. We envisage flux tubes in the dusk sector in the general subcorotation flow in the outer magnetospheres at Jupiter and Saturn moving tailward with speed V, and consider the condition under which they will continue to stretch out down-tail with comparable speed rather than to rotate around the planet via midnight into the dawn sector. Assuming that such a down-tail flow becomes established, the situation is as sketched in Figure 1a, where a near field-aligned down-tail flow of speed V and number density n stretches out closed flux tubes with lesser down-tail speed V_F. Here we are assuming that the thermal velocities of the heavy ions in the outer dusk magnetosphere are not large compared with the bulk velocity V, a condition that should be reasonably satisfied at both Jupiter and Saturn. Figure 4 of *Bagenal and Delamere* [2011]) shows, for example, that the heavy ion thermal velocities in this regime will generally be ~100 km s^{-1} or less, while the bulk speeds are generally larger than this as discussed in section 3.2 below. In Figure 1a the incident plasma particles stream into the central current sheet and are reflected from it or transmitted through it with a lesser speed, the reduced energy principally of the ions being stored in the extending magnetic structure. Assuming for simplicity a one-dimensional current sheet with cold field-aligned plasma beams on either side of the current layer, the momentum balance condition in the field line rest frame moving down-tail with speed V_F is that the field-aligned plasma speed in this frame must have the value

$$V^* = V_A = \frac{B}{\sqrt{2\mu_o m_i n}} \quad , \tag{1}$$

where the Alfvén speed V_A is based on the field strength B outside the current sheet, essentially the field strength in the tail lobe, and the total plasma density $2n$ of the inflow and outflow plasmas combined [e.g., *Cowley and Southwood*, 1980]. We note that equation (1) expresses the marginal firehose stability condition under the conditions stated. In the planetary frame, the field lines are then stretched out down-tail away from the planet provided the flow speed in the planetary frame satisfies $V > V^*$, equivalent to $V > V_A$. If this condition is not met, i.e., if $V < V_A$, such flux tubes would instead move back towards the planet and continue to participate in the sub-corotation flow rather than to stretch out down-tail. For a given value of the tailward flow speed V, essentially the plasma sub-corotation speed in the outer equatorial dusk sector magnetosphere, the condition $V > V_A$ for down-tail stretching is equivalent to requiring the plasma number density to satisfy $n > n^*$, where

$$n^* = \frac{B^2}{2\mu_o m_i V^2} \quad . \tag{2}$$

In other words, for a given down-tail plasma velocity V, the flux tubes have to be sufficiently mass-loaded, $n > n^*$, for outflow to occur. Assuming a transverse field B_θ much smaller than the lobe field B, the speed of the field lines is then given by

$$V_F \approx V - V_A \quad , \tag{3}$$

positive down-tail for $V > V_A$, and negative planetward for $V < V_A$. The down-tail speed of the plasma that has interacted with the current sheet is then $V' \approx V - 2V_A$, which continues to be positive, tailward, if $V > 2V_A$, but will take negative, planetward, values for $V < 2V_A$.

3.2. Consequences for Plasmoid Length at Jupiter and Saturn

At Jupiter, the tail lobe field strength at relevant nightside radial distances ~100 R_J is ~6 nT (see Figure 10 of *Vogt et al*. [2014]), and although the plasma speed in the outer dusk sector is not thoroughly explored to date it seems reasonable to take $V \approx 350$ km s^{-1} [e.g., *Kane et al*., 1995; *Krupp et al*., 2004]. The limiting number density given by equation (2) for mass 20 ions is then $n^* \approx 0.0035\,\mathrm{cm}^{-3}$, such that with typical plasma sheet number densities ~0.01-0.02 cm^{-3} noted above the condition that such outer dusk flux tubes will be stretched out down-tail by the plasma flow should be well satisfied. The Alfvén speed given by equation (1) is then ~150 km s^{-1}, such that the down-tail speed of the closed flux tubes given by equation (3) is ~200 km s^{-1}. Taking an event recurrence time of ~15 h as in section 2.1 then shows that in the interval between disconnection events such flux tubes will have extended a down-tail distance of ~150 R_J, while the subcorotation azimuthal motion of the field line feet in the ionosphere will at least be partially maintained by the atmospheric torque. The implication therefore is that the full structures disconnected in each event will typically be ~150 R_J long, a factor of ten times the ~15 R_J plasmoid length inferred in section 2.1.

Similarly for Saturn, the tail lobe field strength at relevant radial distances ~50 R_J is ~2 nT (see Figure 6 of *Jackman et al*. [2014]), and the plasma speed in the outer dusk sector is $V \approx 150$ km s^{-1} [*Thomsen et al*., 2014]. The limiting number density given by equation (2) for mass 16 ions is then $n^* \approx 0.0026\,\mathrm{cm}^{-3}$, such that with plasma sheet number densities ~0.03 cm^{-3} noted in section 2.2, the condition that the flux tubes will be stretched out down-tail by the mass-loaded plasma flow will again be well satisfied. The Alfvén speed given by equation (1) is then ~50 km s^{-1}, such that the down-tail speed of the flux tubes given by equation (3) will be ~100 km s^{-1}. In the ~45 h between Saturn events such flux tubes will thus have stretched ~250 R_S down-tail, so that the full structures disconnected by the events will be of comparable length, in this case a factor of ~15 longer than the inferred typical plasmoid length of ~15 R_S.

3.3. Physical Picture of the Observed Events

The physical picture of the events observed by Galileo at Jupiter and Cassini at Saturn which we envisage is shown in Figure 1b, where we specifically consider conditions in the central and dawn-sector tail where the down-tail flow V may have ceased or be significantly reduced. A reconnection event within the plasma sheet is then taken to disconnect the distended field lines stretching far down-tail as discussed above, which causes these field lines to contract tailward, accelerating and heating the plasma sheet plasma as they do so. Within the simple one-dimensional current sheet theory presented above, the tailward field line contraction speed tailward of the reconnection site is $V_F = V_A + V$, while the accelerated plasma streams tailward out of the current sheet at speed $V' = 2V_A + V$. The contracted field lines and hot accelerated plasma forms a tailward-propagating bulge within the plasma sheet which at points lying tailward of the reconnection site is observed as a tailward-propagating "plasmoid" with its characteristic bipolar B_θ field signature (or TCR). However, from the above discussion it is evident that this perturbed region represents only a fraction of the whole structure that is disconnected and will eventually be lost to the system down-tail. If reconnection continues onto lobe field lines outside the plasma sheet, an extended interval of tailward-flowing post-plasmoid plasma sheet (PPPS) will also follow the true "plasmoid" interval, as generally observed at both Jupiter and Saturn [*Vogt et al.*, 2014; *Jackman et al.*, 2014]. In Figure 1b the red dots represent the pre-existing plasma sheet plasma as shown in Figure 1a, while the over-lying accelerated lobe plasma forming the PPPS is shown by the green dots. In general these plasmas would be expected to have differing compositions, principally planetary for the "plasmoid" and solar wind for the PPPS.

On the planetward side of the reconnection site a "dipolarization front" is similarly launched towards the planet, as also shown in Figure 1b. Within the one-dimensional current sheet theory the planetward field line contraction speed is $V_F = V_A - V$, while the accelerated plasma streams planetward out of the current sheet with speed $V' = 2V_A - V$. However, both of these quantities may take negative values indicating tailward flow if the tailward plasma flow V is sufficiently large. In this case, however, down-tail stretching of the closed flux tubes would resume, rather than field dipolarization and planetward field line contraction as illustrated. In the latter case, the field structure in the mid-tail regime as depicted is expected to have similar features to that on the tailward side of the reconnection site, with a bipolar B_θ field perturbation propagating planetward associated with a hot plasma "bulge", in which the leading negative B_θ perturbation is less well developed than the following positive perturbation. Such perturbations could be interpreted as a planetward-propagating "plasmoid" despite consisting wholly of perturbed closed field lines. The positive B_θ perturbation is then expected to dominate as the contracting flux tubes begin to interact with the inner sub-corotating plasma-field structures and their inward motion slows.

Two simple corollaries follow from the above physical picture. First, this scenario provides a natural explanation for the asymmetry generally observed in the bipolar B_θ field perturbation transverse to the plasma sheet. For a fully-formed closed-loop plasmoid the positive and negative perturbations should on average be near-symmetric, though variable from case to case depending on the detailed trajectory of the spacecraft through the structure. However, at both Jupiter and Saturn the leading positive perturbation is usually weaker than the trailing negative perturbation, such that in superposed-epoch studies the former is much attenuated relative to the latter in the Jupiter events studied by *Vogt et al*. [2014], and disappears altogether in the Saturn events studied by *Jackman et al*. [2014]. For the picture shown in Figure 1b, however, there is no requirement of approximate symmetry, but rather the positive perturbation in the leading part of the plasma sheet bulge will generally be less developed than the trailing negative perturbation, as observed. This asymmetry would be expected to gradually disappear with distance down-tail, however, with the magnetic structures becoming on average symmetric at down-tail distances beyond a few hundred planetary radii where the full plasmoid structure is observed. This regime has not been explored to date by any spacecraft equipped with a magnetic field experiment.

Second, it is predicted that the apparent length of the plasmoid structure will increase with down-tail distance from the reconnection site, corresponding in general to some reasonable fraction of the latter distance, up to the point where the full structure is observed at distances beyond a few hundred planetary radii. Given the expected natural variability in position of the reconnection site, however, observations over a significant range of distances comparable to the latter will probably be required to reveal this dependence. Beyond such distances full plasmoids of ~100 R_J length travelling down Jupiter's tail at ~400 km s^{-1}, say, would produce ~5 h bursts of plasma that might account for some of the plasma structures reported in the New Horizons spacecraft ion data at distances of ~500-1500 R_J [*McComas et al.*, 2007]. Of course, lacking magnetic measurements, it is impossible to be clear about the true nature of these events. Plasmoid structures ~150-200 R_S long travelling down Saturn's far tail at ~300 km s^{-1} would similarly produce plasma bursts of ~10 h duration.

The most important point here, however, is that if the plasma conditions in the extended disconnected structure are similar to those observed within the near-planet "plasmoid", the total plasmoid mass and mass-loss rates discussed in section 2 will represent under-estimates typically by an order of magnitude or more. Thus a typical mass loss rate of ~30 kg s^{-1} estimated for the Jupiter system in section 2.1 becomes ~300 kg s^{-1}, now of similar order to the Io plasma production rate of ~500-1000 kg s^{-1}, while similarly a typical mass loss rate of ~7 kg s^{-1} estimated for Saturn in section 2.2 becomes at least ~70 kg s^{-1}, now well within the range of the estimated Enceladus plasma production rates of ~50-150 kg s^{-1}. We thus conclude that on the picture presented here, the observed plasmoid occurrence rates in the Jupiter and Saturn systems may be fully capable of removing internally-generated plasma mass at rates comparable to the estimated moon production rates, such that there may not be need of any "hidden", e.g., small scale, processes that operate at competitive rates.

4. Summary and Conclusions

In this paper we have considered estimates of the mass-loss rates due to plasmoids propagating down-tail in Jupiter's and Saturn's magnetospheres based on the plasmoid properties and occurrence statistics discussed by *Vogt et al*. [2014] for Jupiter and *Jackman et al*. [2014] for Saturn. Typical values are estimated as ~30 kg s^{-1} for Jupiter based on large-scale structures that recur on time scales of ~15 h, and ~7 kg s^{-1} for Saturn based similarly on large-scale structures that recur on time scales of ~45 h. In both cases these values fall short of moon plasma production sources by around an order of magnitude, estimated as typically ~500-1000 kg s^{-1} for Io at Jupiter and ~50-150 kg s^{-1} for Enceladus at Saturn. We point out, however, that on the above recurrence time-scales the outflow of mass-loaded closed flux tubes into the tail should reach down-tail distances far exceeding those corresponding to the distances where the above plasmoids signatures were observed. Specifically, from outflow speeds based on plasma observations in the outer dusk sectors of these magnetospheres we estimate that at Jupiter mass-loaded flux tubes will reach ~250 R_J down-tail on ~15 h recurrence time scales, compared with ~100 R_J observation distances for the Galileo measurements reported by *Vogt et al*. [2014], the latter typically being within a few tens of R_J of the reconnection site. Similarly at Saturn we estimate that such flux tubes will reach ~300 R_S down-tail on the ~45 h recurrence time scale, compared with ~30-65 R_S radial distances for the Cassini measurements reported by *Jackman et al*. [2014], again at most a few tens of R_S from the reconnection site. In such cases the "plasmoid" structures observed, of order ~10 planetary radii long, represent only the tailward-contracting near-planet portions of the overall distended structures that are disconnected by these reconnection events. On the above estimates the overall structures are at least an order of magnitude longer, with a consequent overall mass-loss which is an order of magnitude larger than those based on the observed perturbed structures. The above values of the plasmoid mass-loss rates then transform to ~300 kg s^{-1} for Jupiter and ~70 kg s^{-1} for Saturn, now comparable with the above moon sources. On this basis the observed plasmoid events may be fully capable of removing the bulk of the moon-injected plasma, such that there is no requirement for "hidden" small-scale processes of comparable efficacy, such a "micro-plasmoids" or transmission through the magnetopause by some, e.g., finite-gyroradius, process.

We further point out that the picture presented provides a natural explanation for the observed asymmetry in the bipolar perturbation field transverse to the plasma sheet in the observed "plasmoids", in which the leading positive deflection is generally and on average considerably weaker than the following negative deflection. It also predicts that the apparent plasmoid lengths observed in these systems will grow with distance down-tail from the reconnection sites to a full size of ~100-200 planetary radii at distances exceeding ~300 planetary radii down-tail, though given the likely natural variability in location of the reconnection sites, observations over a substantial fraction of such distances will be required to confirm this effect. Such structures propagating down-tail at a few hundred km s^{-1} would give rise to several-hour bursts of plasma at larger distances, possibly related to the ion bursts observed by New Horizons at distances of ~500-1500 R_J down the Jovian tail.

Acknowledgement. SWHC was supported by STFC grant ST/K001000/1. JDN and CMJ were supported by STFC Advanced and Ernest Rutherford Fellowships, respectively.

References

Bagenal, F. (2007), The magnetosphere of Jupiter: Coupling the equator to the poles, *J. Atmos. Sol. Terr. Phys*., *69*, 387-402, doi:10.1016/j.jastp.2006.08.012.

Bagenal, F., and P. A. Delamere (2011), Flow of mass and energy in the magnetospheres of Jupiter and Saturn, *J. Geophys. Res.*, *116*, A05209, doi:10.1029/2010JA016294.

Bunce, E. J., S. W. H. Cowley, D. M. Wright, A. J. Coates, M. K. Dougherty, N. Krupp, W. S. Kurth, and A. M. Rymer (2005), In situ observations of a solar wind compression-induced hot plasma injection in Saturn's tail, *Geophys. Res. Lett.*, *32*, L20S04, doi:10.1029/2005GL022888.

Chen, Y., and T. W. Hill (2008), Statistical analysis of injection/dispersion events in Saturn's inner magnetosphere, *J. Geophys. Res.*, *113*, A07215, doi:10.1029/2008JA013166.

Chen, Y., T. W. Hill, A. M. Rymer, and R. J. Wilson (2010), Rate of radial transport of plasma in Saturn's inner magnetosphere, *J. Geophys. Res.*, *115*, A10211, doi:10.1029/2010JA015412.

Cowley, S. W. H., and D. J. Southwood (1980), Some properties of a steady-state geomagnetic tail, *Geophys. Res. Lett.*, *7*, 833-836.

Cowley, S. W. H., E. J. Bunce, and T. S. Stallard, and S. Miller (2003), Jupiter's polar ionospheric flows: Theoretical interpretation, *Geophys. Res. Lett.*, *30*(5), 1220, doi:10.1029/2002GL016030.

Delamere, P. A., and F. Bagenal (2010), Solar wind interaction with Jupiter's magnetosphere, *J. Geophys. Res.*, *115*, A10201, doi:10.1029/2010JA015347.

Fleshman, B. L., P. A. Delamere, F. Bagenal, and T. Cassidy (2013), A 1-D model of physical chemistry in Saturn's inner magnetosphere, *J. Geophys. Res.*, *118*, 1567–1581, doi:10.1002/jgre.2010.

Frank, L. A., W. R. Paterson, and K. K. Khurana (2002), Observations of thermal plasmas in Jupiter's magnetotail, *J. Geophys. Res.*, *107*(A1), 1003, doi:10.1029/2001JA000077.

Hill, T. W., A. M. Rymer, J. L. Burch, F. J. Crary, D. T. Young, M. F. Thomsen, D. Delapp, N. Andre, A. J. Coates, and G. R. Lewis (2005), Evidence for rotationally driven plasma transport in Saturn's magnetosphere, *Geophys. Res. Lett.*, *32*, L14S10, doi:10.1029/2005GL022620.

Hill, T. W., M. F. Thomsen, M. G. Henderson, R. L. Tokar, A. J. Coates, H. J. McAndrews, G. R. Lewis, D. G. Mitchell, C. M. Jackman, C. T. Russell, M. K. Dougherty, F. J. Crary, and D. T. Young (2008), Plasmoids in Saturn's magnetotail, *J. Geophys. Res.*, *113*, A01214, doi:10.1029/2007JA012626.

Jackman, C. J., C. T. Russell, D. J. Southwood, C. S. Arridge, N. Achilleos, and M. K. Dougherty (2007), Strong rapid dipolarizations in Saturn's magnetotail: In situ evidence of reconnection, *Geophys. Res. Lett.*, *34*, L11203, doi:10.1029/2007GL029764.

Jackman, C. J., C. S. Arridge, N. Krupp, E. J. Bunce, D. G. Mitchell, H. J. McAndrews, M. K. Dougherty, C. T. Russell, N. Achilleos, G. H. Jones, and A. J. Coates (2008), A multi-instrument view of reconnection at Saturn, *J. Geophys. Res.*, *113*, A11213, doi:10.1029/2008JA013592.

Jackman, C. J., J. A. Slavin, and S. W. H. Cowley (2011), Cassini observations of plasmoid structure and dynamics: Implications for the role of magnetic reconnection in magnetospheric circulation at Saturn, *J. Geophys. Res.*, *116*, A10212, doi:10.1029/2011JA016682.

Jackman, C. J., J. A. Slavin, M. G. Kivelson, D. J. Southwood, N. Achilleos, M. F. Thomsen, G. A. DiBraccio, J. P. Eastwood, M. P. Freeman, M. K. Dougherty, and M. F. Vogt (2014), Saturn's dynamic magnetotail: A comprehensive magnetic field and plasma survey of plasmoids and traveling compression regions and their role in global magnetospheric dynamics, *J. Geophys. Res.*, *119*, 5465-5494, doi:10.1002/2013JA019388.

Jackman, C. J., M. F. Thomsen, D. G. Mitchell, N. Sergis, C. S. Arridge, M. Felici, S. V. Badman, C. Paranicas, X. Jia, G. B. Hospodarsky, M. Andriopoulou, K. K. Khurana, A. W. Smith, and M. K. Dougherty (2015), Field dipolarization in Saturn's magnetotail with planetward ion flows and energetic particle flow bursts: Evidence of quasi-steady reconnection, *J. Geophys. Res.*, *120*, in press, doi:10.1002/2015JA020995.

Kane, M., B. H. Mauk, E. P. Keath, and S. M. Krimigis (1995), Hot ions in Jupiter's magnetodisc: A model for Voyager 2 Low-Energy Charged Particle measurements, *J. Geophys. Res.*, *100*, 19473-1946.

Kasahara, S., E. A. Kronberg, T. Kimura, C. Tao, S. V. Badman, A. Masters, A. Retinò, N. Krupp, and M. Fujimoto (2013), asymmetric distribution of reconnection jet fronts in the Jovian nightside magnetosphere, *J. Geophys. Res.*, *118*, 375-384, doi:10.1029/2012JA018130.

Khurana, K. K., and H. K. Schwarzl (2005), Global structure of Jupiter's magnetospheric current sheet, *J. Geophys. Res.*, *110*, A07227, doi:10.1029/2004JA010757.

Kivelson, M. G., and K. K. Khurana (1995), Models of flux ropes embedded in a Harris neutral sheet: Force-free solutions in low and high beta plasmas, *J. Geophys. Res.*, *100*, 23,637-23,645.

Kivelson, M. G., and D. J. Southwood (2005), Dynamical consequences of two modes of centrifugal instability in Jupiter's outer magnetosphere, *J. Geophys. Res.*, *110*, A12209, doi:10.1029/2005JA011176.

Kronberg, E. A., J. Woch, N. Krupp, A. Lagg, K. K. Khurana, and K.-H. Glassmeier (2005), Mass release at Jupiter: Substorm-like processes in the Jovian magnetotail, *J. Geophys. Res.*, *110*, A03211, doi:10.1029/2004JA010777.

Kronberg, E. A., K.-H. Glassmeier, J. Woch, N. Krupp, A. Lagg, and M. K. Dougherty (2007), A possible intrinsic mechanism for the quasi-periodic dynamics of the Jovian magnetosphere, *J. Geophys. Res.*, *112*, A05203, doi:10.1029/2006JA011994.

Kronberg, E. A., J. Woch, N. Krupp, and A. Lagg (2008a), Mass release process in the Jovian magnetosphere: Statistics on particle burst parameters, *J. Geophys. Res.*, *113*, A10202, doi:10.1029/2008JA013332.

Kronberg, E. A., J. Woch, N. Krupp, A. Lagg, P. W. Daly, and A. Korth (2008b), Comparison of periodic substorms at Jupiter and Earth, *J. Geophys. Res.*, *113*, A04212, doi:10.1029/2007JA012880.

Krupp, N., V. M. Vasyliunas, J. Woch, A. Lagg, K. K. Khurana, B. H. Mauk, D. J. Williams, S. M. Krimigis, W. S. Kurth, L. A. Frank, and W. R. Paterson (2004), Dynamics of the Jovian magnetosphere, in *Jupiter: The Planet, Satellites, and Magnetosphere*, edited by F. Bagenal et al., pp. 617-638, Cambridge Univ. Press, New York.

Mauk, B. H., D. C. Hamilton, T. W. Hill, G. B. Hospodarsky, R. E. Johnson, C. Paranicas, E. Roussos, C. T. Russell, D. E. Shemansky, E. C. Sittler Jr., and R. M. Thorne (2009), Fundamental processes in Saturn's magnetosphere, in *Saturn from Cassini-Huygens*, edited by M. K. Dougherty, L. W. Esposito, and S. M. Krimigis, pp. 281-331, Springer, New York.

McComas, D. J., F. Allegrini, F. Bagenal, F. Crary, R. W. Ebert, H. Elliott, A. Stern, and P. Valek (2007), Diverse plasma populations and structures in Jupiter's magnetotail, *Science*, *318*, 217-220.

Thomsen, M. F., C. M. Jackman, R. L. Tokar, and R. J. Wilson (2014), Plasma flows in Saturn's nightside magnetosphere, *J. Geophys. Res.*, *119*, 4521-4535, doi:10.1002/2014JA019912.

Thomas, N., F. Bagenal, T. W. Hill, and J. K. Wilson (2004), The Io neutral cloud and plasma torus, in *Jupiter: The Planet, Satellites, and Magnetosphere*, edited by F. Bagenal et al., pp. 561-591, Cambridge Univ. Press, New York.

Vasyliunas, V. M. (1983), Plasma distribution and flow, in *Physics of the Jovian Magnetosphere*, edited by A. J. Dessler, pp. 395-453, Cambridge Univ. Press, New York.

Vogt, M. F., M. G. Kivelson, K. K. Khurana, S. P. Joy, and R. J. Walker (2010), Reconnection and flows in the Jovian magnetotail as inferred from magnetometer observations, *J. Geophys. Res.*, *115*, A06219, doi:10.1029/2009JA015098.

Vogt, M. F., C. M. Jackman, J. A. Slavin, E. J. Bunce, S. W. H. Cowley, M. G. Kivelson, and K. K. Khurana (2014), Structure and statistical properties of plasmoids in Jupiter's magnetotail, *J. Geophys. Res.*, *119*, 821-843, doi:10.1002/2013JA019393.

Woch, J., N. Krupp, and A. Lagg (2002), Particle bursts in the Jovian magnetosphere: Evidence for a near-Jupiter neutral line, *Geophys. Res. Lett.*, *29*(7), 1138, doi:10.1029/2001GL014080.

Figure Caption

Figure 1. Sketches illustrating the plasma sheet states discussed. (a) Down-tail stretching of the plasma sheet field lines at speed V_F by a down-tail plasma flow of speed V, related by equation (3). The plasma sheet region is indicated by the red dots, surrounded on either side by the tail lobes. (b) Effect of a reconnection event within the plasma sheet in a region of reduced down-tail flow, showing planetward propagation of the field lines on the planetary side of the reconnection site forming a "dipolarization front", and tailward propagation of contracted field lines on the other side forming a tailward-propagating "plasmoid" head magnetically connected to a structure that extends far down-tail. The red dotted region shows the plasma originating in the pre-existing plasma sheet as in panel (a), while the green dotted region represents accelerated tail lobe plasma that overlays this structure if reconnection continues onto lobe field lines, forming a plasma sheet boundary layer on the planetward side of the reconnection site and the PPPS on the tailward side. The speed of the accelerated plasma V' is as given in section 3.3.

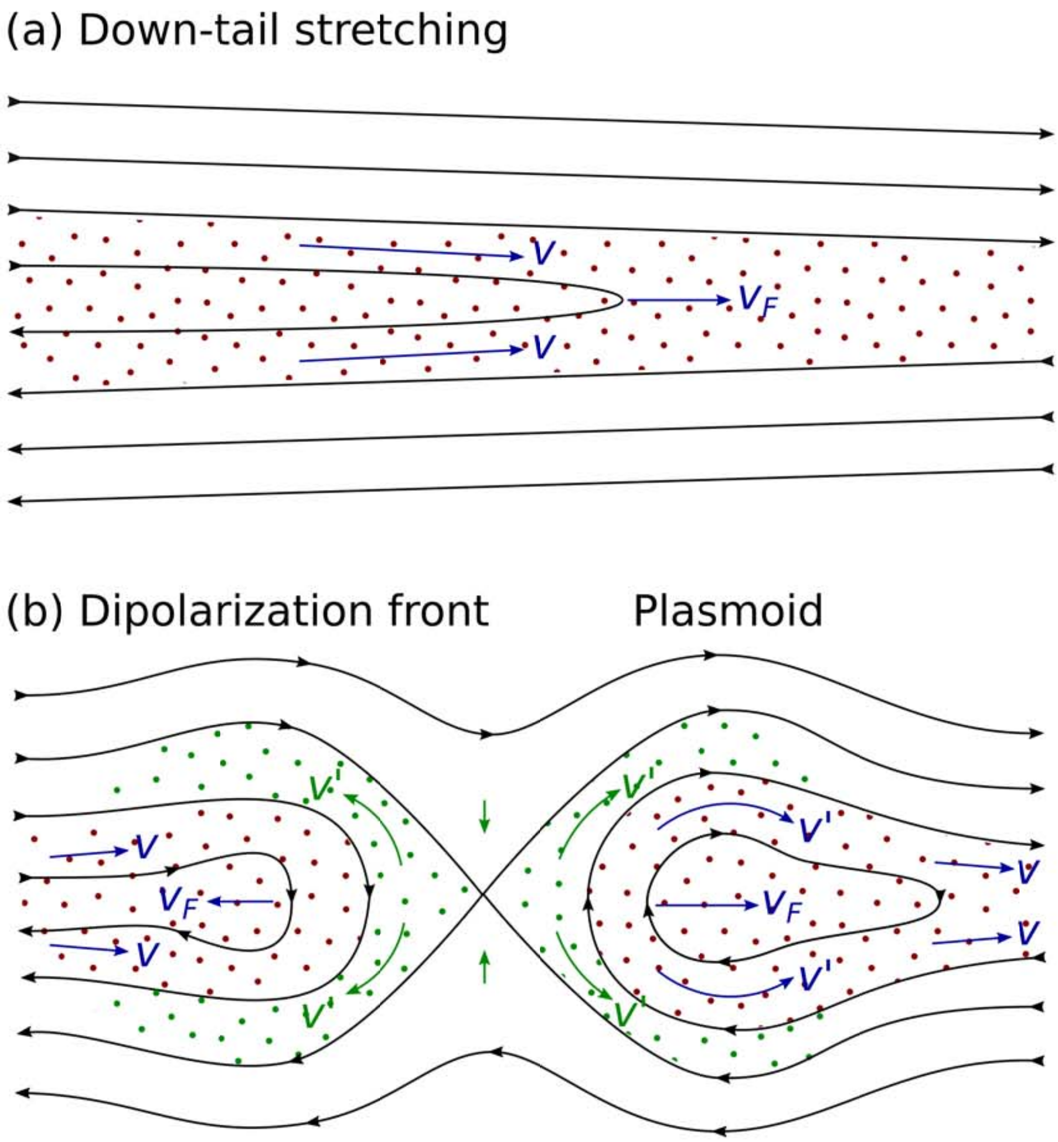
(a) Down-tail stretching
V
V_F
V
(b) Dipolarization front
Plasmoid
V'
V
V_F
V
V'
V'
V'
V'
V
V_F
V
V'
V'

Figure 1